Journal of Renewable Materials
DOI:10.32604/jrm.2020.08696
Article

Tech Science Press

Frequencies Prediction of Laminated Timber Plates Using ANN Approach

Jianping Sun[1], Jan Niederwestberg[2,*], Fangchao Cheng[1] and Yinghei Chui[2]

[1]School of Resources, Environment and Materials, Guangxi University, Nanning, 530004, China
[2]Department of Civil and Environmental Engineering, University of Alberta, Edmonton, AB, T6G 1H9, Canada
*Corresponding Author: Jan Niederwestberg. Email: Jan.niederwestberg@ualberta.ca
Received: 26 September 2019; Accepted: 13 January 2020

Abstract: Cross laminated timber (CLT) panels, which are used as load bearing plates and shear panels in timber structures, can serve as roofs, walls and floors. Since timber is construction material with relatively less stiffness, the design of such structures is often driven by serviceability criteria, such as deflection and vibration. Therefore, accurate vibration and elastic properties are vital for engineered CLT products. The objective of this research is to explore a method to determine the natural frequencies of orthotropic wood plates efficiently and fast. The method was developed based on vibration signal processing by wavelet to acquire the effective sample data, and a model developed by artificial neural network (ANN) to achieve the prediction of nature frequencies. First, experiments were performed to obtain vibration signals of single-layer plates. The vibration signals were then processed by wavelet packet transform to extract the eigenvectors, which served as the samples to train the ANN model. The trained model was employed to predict three nature frequencies of other test specimens. The results showed that the proposed method can produce predicted frequencies fast and efficiently within 10% of the measured values.

Keywords: Cross laminated timber (CLT); vibration test; natural frequency; wavelet analysis; artificial neural network (ANN)

1 Introduction

Cross laminated timber (CLT) is a panel-shaped wood product, assembled of cross-wise oriented layers of lamellas (commonly softwood) which, compared to the raw material, benefits from homogenized mechanical properties. As an engineered product, CLT can contribute not only to save wood resource but also to enable a large-scale wood construction. Moreover, CLT has emerged as a promising alternative to concrete in large building structures. The replacement of concrete slabs with CLT plates in new buildings creates market opportunities for wood industry. The value of the global CLT market was estimated at $1.6 billion in 2024 [1]. To meet the demands for structural capacities in large structures, attempts should be made to improve the product characteristics of CLT [2-4]. The design of CLT structure is often governed by serviceability criteria such as deflection and vibration. Hence, accurate measurement of its elastic constants is critical to ensure satisfactory structural performance of CLT structures.

The current test methods for measuring elastic properties of CLT panels are largely based on static bending test procedure such as ASTM D198 [5] by using CLT strips and testing them as beams [6]. These static beam test methods can only measure one elastic property from one test. In construction, CLT panels can be utilized as two-way plates, but in structural designs they are treated as beam elements. Therefore the benefits of the two-way plate action are not currently realized. This requires the measurement of elastic moduli in the two orthogonal directions. To measure these two properties, it is more efficient to test CLT as a plate utilizing vibration test techniques. As a nondestructive testing method, vibration method is used to study the performance of CLT material, such as damping ratios for CLT panels [7], dynamic MOE of CLT by tap tone [8,9], longitudinal vibration [10] and transverse vibration [11], and CLT gluing by Ultrasonic Testing [12], natural frequencies and mode shapes of CLT [13].

Meanwhile, much attention was paid also to modal analysis method [14], which is a dynamical means to evaluate the modal properties by vibration test. Vibration modal analysis method was employed to estimate natural frequencies of CLT materials [15,16] and four-story CLT building [17,18]. The application of modal analysis to determine the elastic constants of orthotropic plate was attempted by Deobald et al. [19]. A theoretical approach relating natural frequencies of an orthotropic plate to its elastic and physical properties has been presented by Leissa [20]. This approach formed the theoretical basis of subsequent research to measure elastic properties of orthotropic plates from modal testing results. Sobue et al. [21] were among the first researchers to apply a similar approach to wood-based plate specimens. They presented a vibration method to measure the moduli of elasticity in the major and minor direction, E11 and E22 respectively, as well as the modulus of rigidity G12 of plywood panels. Gsell et al. [22] and Steiger et al. [23] derived stiffness properties of CLT by a new developed method, which is based on experimental and theoretical modal analysis. Research conducted by Czaderski et al. [24] and Steiger et al. [25] showed that modal test could be used to assess CLT stiffness properties derived from bending tests of strip-shaped specimens cut from gross panels. A subsequent research demonstrated that vibration modal analysis is an effective method to determine the vibration constants of CLT panels [25], but such tests suffer from being time-consuming and tedious and are not in all cases a reliable indicator of the CLT's real mechanical performance. More recently, Zhou et al. [26,27] developed a modal testing technique with a unique algorithm to extract the required natural frequencies to calculate up to 5 elastic constants of mass timber panels such as CLT, namely the two bending moduli and three shear moduli. Even though the technique developed by Zhou et al. [27] is a big improvement over previous methods by [24] and [25] in terms of time and efficiency, some degree of user intervention, such as identification of appropriate vibration modes for calculation as is discussed below, is still required.

A review of previous research suggests that since there is a need to correctly identify several vibration modes, the application of modal analysis to test orthotropic plates is often tedious and time-consuming. This is because construction of mode shape requires testing the panel at a number of locations and the organization of the modal displacement data. The aim of the research project presented here was to develop a technique that identifies the natural frequencies without the need to construct mode shapes, using artificial neural network (*ANN*) approach.

2 Materials and Methods

2.1 Preparation of Single-Layer Panels and Vibration Test

The wood panels investigated here were made of spruce (*Picea spp*.) boards which were stored for several months in a conditioning chamber at a temperature of 20°C and a relative humidity of 65%. After that they were planed to a thickness of 19 mm and trimmed to a length of 1500 mm. Then a modal test method developed by Chui [28,29] was employed to measure the first two natural frequencies of each board. Based on which and the density the modulus of elasticity (MOE) and the shear modulus of each board were calculated. Boards with similar properties including growth ring orientation, density, MOE

were grouped and then ripped to provide 3 groups of laminates with a width of 120 mm, 76 mm and 32 mm respectively. Boards with similar properties and the same width were edge-glued to single-layer panels using a polyurethane adhesive. After the gluing process the planes were re-sized to uniform dimensions of 1220 mm × 588 mm × 15.4 mm. A total of 55 single-layer panels were prepared and tested in this study.

Next, 55 single-layer panels were conducted by vibration test in free-free boundary conditions (FFFF) where a single-layer panel was hung vertically by thin, lightweight threads and was excited with the hammer at two points located at the upper left and lower right a grid of 6 by 6 equally spaced points. The dynamic vibration response was detected by an accelerometer located on the opposite side of the panel, as shown in Fig. 1. Vibration equipment was used for the test, which consists of an instrumented hammer, accelerometer, a dynamic signal analyser and the modal analysis software installed in a laptop computer.

Finally, the signals were digitized and introduced to an analysis program of wavelet packed transform, which was developed in MATLAB program language by the first author, to obtain the decomposed signals in time and frequency domain simultaneously. Vibration modes and three natural frequencies: f_{11}, f_{12} and f_{31} were performed in another study by Niederwestberg et al. [30] and were further analyzed in this study.

2.2 Wavelet Analysis of Vibration Signals

In order to extract signals with special frequency bands, an algorithm was adopted to reconstruct the expected signals by the coefficient after decomposing using the wavelet packet. Here, wavelet packet transform (WPT), which was an exciting extension of the wavelet transform, was employed to decompose the vibration signals. Based on orthogonal direct sum decomposition of orthogonal wavelet function space $L^2(R)$, the idea of WPT was formed in the combination of multi-resolution analysis and orthogonal wavelet constructed. Wavelet packet transform is defined as the space of the wavelet packet, as shown in Eq. (1):

$$U_j^l = closespan\left\{ U_{l,j,n}(t) = 2^{-\frac{j}{2}} U_l\left(2^{-j}t - n\right) \quad n \in Z \right\} \tag{1}$$

where U is the space of the wavelet packet. The WPT of the signal $f(t) \in L^2(R)$ is defined by Eq. (2):

$$d_{j,\,n}^{(l)} = \left\langle f(t),\ U_{l,j,\,n}(t) \right\rangle = 2^{-j/2} \int_{-\infty}^{+\infty} f(t)\overline{U_l(2^{-j}t - n)} \tag{2}$$

The algorithm of MATLAB decomposition corresponding to the transform is shown below in Eq. (3):

$$\begin{cases} d_{j,\,n}^{(2l)} = \sum\limits_{m \in Z} \overline{h_{m-2n}} d_{j-1,}^{l} \\ d_{j,\,n}^{(2l+1)} = \sum\limits_{m \in Z} \overline{g_{m-2n}} d_{j-1,\,n}^{l} \end{cases} \tag{3}$$

where d is the decomposed coefficient, h_{m-2n} and g_{m-2n} is low pass filter and high pass filter respectively. The coefficients from WPT were the arbitrary time-frequency resolution of a signal. The vibration signals by vibration test were transformed by a three-level wavelet packet. For the complex vibration signal with finite energy, the energy of each frequency band is the square sum of the wavelet coefficients, and the energy rate of each frequency is the percentage of the total energy. By the characteristic vector composed of each energy rate, the basic characteristics of the signal are not only reflected effectively, but also are reduced in their dimensionality. And the eigenvectors of signals, served as input into ANN model shown in Fig. 1.

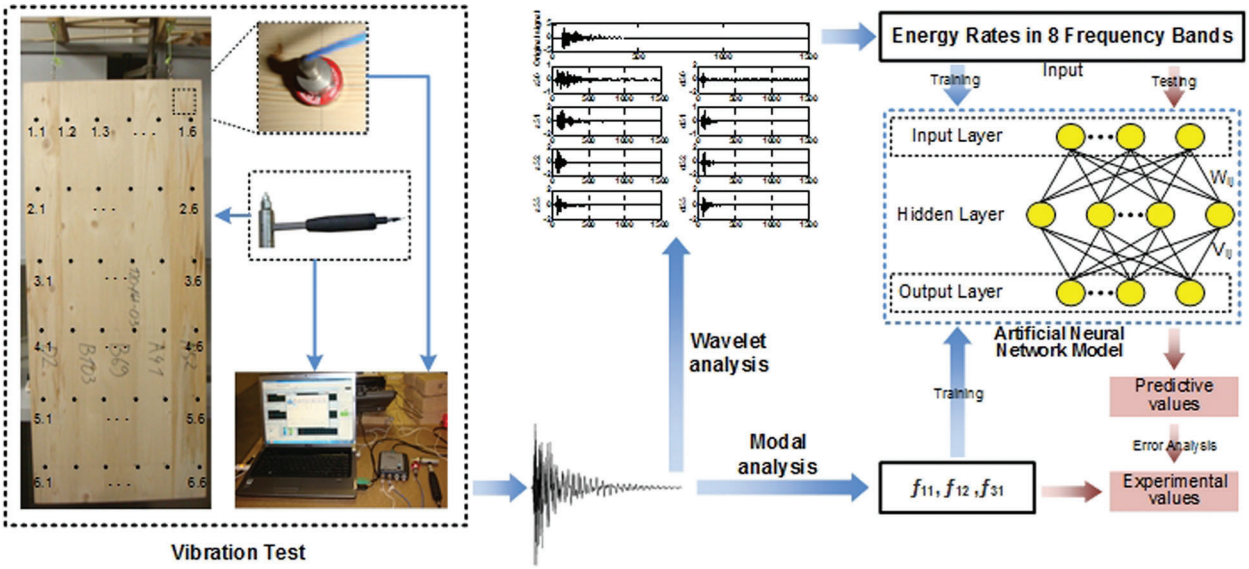

Figure 1: The vibration test, signals processing by WPT and *ANN* model construction

2.3 Developing Model by ANN

ANN, emerged as a new branch of computing, attempts to mimic the structure and operations of biological neural systems. An ANN can be considered as a black box with the capacity to predict an output pattern when it recognizes a given input pattern. The neural network can be seen as a highly nonlinear mapping from input to output, i.e., $F : R_m \rightarrow R_n, f(X) = Y$. For sample collection, the input $x_i(\in R_m)$, the output is $y_i(\in R_n)$ that there is a mapping $g(x_i) = y_i\,(i = 1,\ 2,\ \cdots,\ m)$. The mapping "$f$" that in some sense can be considered as the best approximation of "g". The relationship model can be expressed by Eq. (4).

$$[F] = f_1\left(\sum_{j=1}^{N} \omega_{jk} f_2\left(\sum_{i=1}^{M} \omega_{ij} x_i - \theta_i\right) - \theta_j\right) \tag{4}$$

where ω_{ij} and ω_{jk} are connection weight matrices from the input layer to the hidden layer and from the hidden layer to the output layer. θ_i and θ_j are the threshold vector of hidden layer and output layer respectively. $f_1(x)$ and $f_2(x)$ are the transfer function from input layer to hidden layer and from the hidden layer to output layer.

The topology structure was determined firstly, and back-propagation (BP) neural network was selected as the ANN model architecture in this study. The network model was defined by 8 (8 energy rates of one vibration signal decomposed by WPT) or 16 (16 energy rates of two vibration signal decomposed by WPT) inputs and 3 outputs, corresponding to f_{11}, f_{12} and f_{31} mentioned above. In order to determine the optimal number of nodes in the hidden layer, several network models were built with different number of hidden nodes. There were 15 and 12 hidden nodes for the network with 8 and 16 inputs respectively, which were determined by the best mean square error (MSE) of the network learning performance.

Then, training samples and verifying samples were determined. Among the 55 samples, 44 samples were utilized as the training samples to train the model; and the other 11 samples as verifying samples.

Finally, the *ANN* model was trained and verification. Using back-propagation learning algorithm, different learning performances of these networks were obtained based on MSE. After several training and cross validation processes, the two network models reached their best performances of learning and cross validation.

3 Results and Discussion

3.1 Extracting Feature Vectors of Time Domain Signals

As described above, the signal was decomposed by a 3-level wavelet packet to eight frequency bands. And the percentage of energy per frequency band, that is to say energy rate, was obtained to serve as the training samples to ANN model. Considering the effect of frequency band division and the problem of tight support and computational complexity in time domain, the wavelet packet "db5" was chosen to decompose the original signal into eight different frequency bands shown in Fig. 2. The length of sampling signal was N = 4096 and the sampling frequencies was 750 Hz and the frequency bandwidth of wavelet packet decomposition was 46.875 Hz. Signals were decomposed in the frequency range of [0 Hz 375 Hz]. There were 8 (2^3) equal bandwidths of [0 Hz 46.875 Hz], [46.875 Hz 93.75 Hz], [93.75 Hz 140.625 Hz], [140.625 Hz 187.5 Hz], [187.5 Hz 234.375 Hz], [234.375 Hz 281.25 Hz], [281.25 Hz 328.125 Hz] and [328.125 Hz 375 Hz]. An example of an original and the eight decomposed time signals are shown in Fig. 2. Here, a30, a31, a32 and a33 are the approximations of signals (low frequency) and d30, d31, d32 and d33 are details of signals (high frequency).

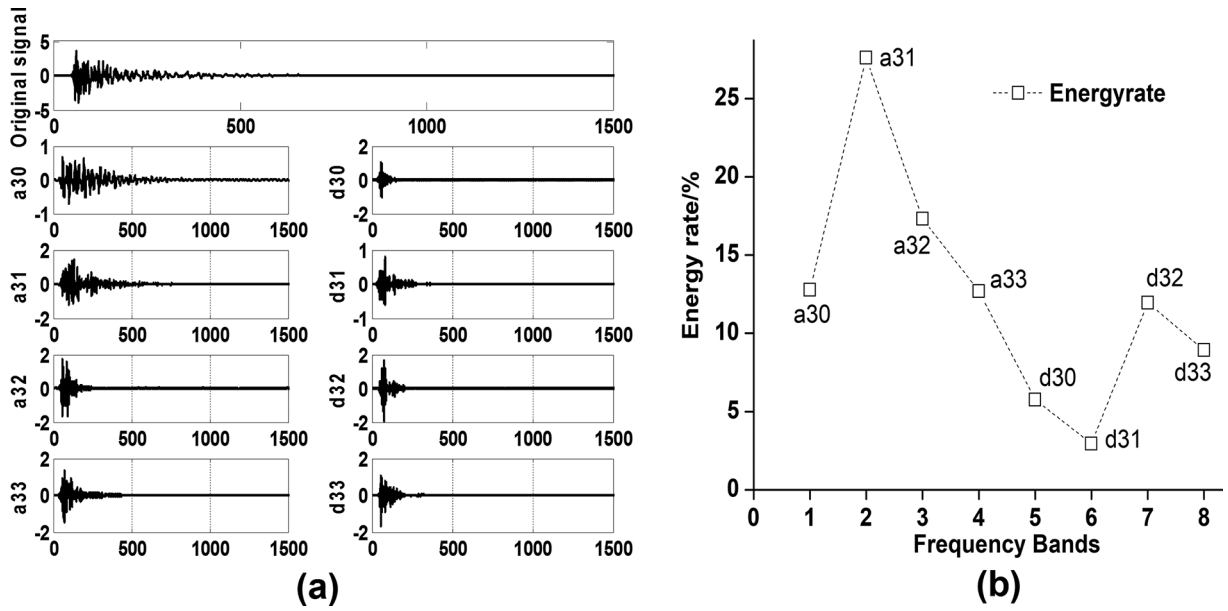

Figure 2: (a) Wavelet packet decomposed for three layers by "db5" wavelet; (b) Energy rate (the percentage of energy per frequency band to total signal energy) in eight frequency bands

The eight energy rates are shown in Fig. 2, from which it is found that the low frequency signals accounted for most of the energy of the original signal and a30 accounted for a 27.6% share of the maximum energy of the signal, while d31 is the minimum in high frequency range with an energy rate of 2.95%. The approximations and details of the signal are 70.41% and 29.59% respectively of the original signal. The eight energy rates in eight frequency bands are able to serve as an eigenvector to describe the nature of the signal. The energy rate varied significantly from 2.95% to 27.6%. All the vibration signals from 55 specimens were processed by the approach mentioned above. For the same specimen, two vibration signals were acquired by tapping the two points of 6.1 and 1.6 as shown in Fig. 1. The energy rate of 6.1 served as the input to train one ANN model, and those of 6.1 and 1.6 for another ANN model.

3.2 Predicting the Natural Frequencies by One-Point Vibrating Signal

As discussed above, a three-layer ANN was built to express the relationship between vibration signals in time domain and the three natural frequencies f_{11}, f_{12} and f_{13}. The topology of the model was 8 neurons, 15 neurons and 3 neurons (8-15-3) for input, hidden and output layers, respectively. The 8-dimension vectors of the signal energy rate of the vibration signal from one excited point of 6.1 shown in Fig. 1 were used as sample data to train ANN model. After determining the network topology and training samples, the network model was trained and it constantly adjusted the network weights matrices and parameters through learning from the given samples until a given acceptable training error was met. With the trained network model the simulation analysis was conducted, the values of correlation coefficient, R, were above 0.93.

The natural frequencies were predicted by the trained network model. And the errors between the three natural frequencies from experiment and those from the ANN prediction ware shown in Fig. 3. It was noted that, for 11 validation samples, the difference on average is about 7.84%, 6.66% and 4.08% for f_{11}, f_{12} and f_{13}, respectively. All the errors were under 20%, but there are 6 prediction error values greater than 10%. For f_{11}, three prediction errors are greater than 10% and all others were less than 10%; while only one error is above 10% for f_{12} and f_{31}.

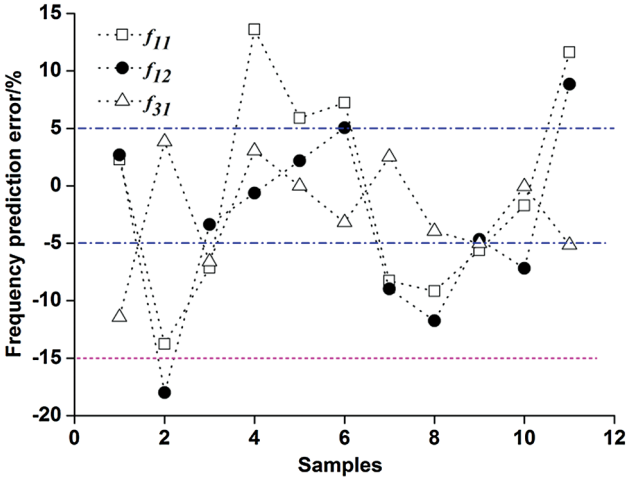

Figure 3: Errors of f_{11}, f_{12} and f_{31} between ANN model with the topology of 8-15-3 and experiment

Regarding the panels consisting of 32 mm wide boards (Samples 1 to 5), four errors were greater than 10%. In comparison only one error was greater than 10% for the boards made with laminate width of 120 mm (Samples 9 to 11), while all errors are less than 10% for the boards made with laminate width of 76 mm (Samples 6 to 8). These were attribute to the wood board width, the wider the width of wood boards were, the more stable the vibration characteristics of the single-layer panel prepared by the wide boards. On the contrary, the narrower the boards were, the greater the variability of the single-layer panel made of those. And it was obvious that the prediction errors by the ANN model, of which energy rates of one excited point of 6.1 served as the input.

3.3 Improving the Generalization of ANN by Two-Point Vibration Signal

Some measures were taken to improve the generalization of ANN model, such as improving the training samples and increasing hidden nodes, which resulted in decrease training time, but insignificant improvement in generalization of the network model. It is partially due to the fact that model generalization was largely dependent on whether the sample data was representative or not, and partially due to the error of verification data. Furthermore, for a sample, the vibration mode shapes could be

obtained by each vibrating signal of the mesh points shown in Fig. 1. The more mesh points were considered, the more accurate the vibration mode shapes were.

Consequently, some attempt was made to improve the ANN generalization by increasing information of sample data. More vibration signals from different points should be employed as the input to train the network model to improve the generalization performance. Therefore, another 8-dimension vector of the vibration signal at the point of "1.6" was also used with the point of "6.1" together as the input to train ANN model. With the the two points of "1.6" and "6.1" discussed above, a 16-dimension vector of energy rate was served as the training samples. Corresponding to it, the topology of the ANN model became 16 neurons, 12 neurons and 3 neurons (16-12-3) for input, hidden and output layers, respectively, and the neuron nodes in the hidden layer were determined by the way described above.

Same as the above neural network model training, 44 training samples and 11 samples for verification, after being trained well, the ANN model was used to predict three natural frequencies. And the f_{11}, f_{12} and f_{13} from experiment and ANN prediction were shown in Figs. 4a–4c. By comparing the experimental and

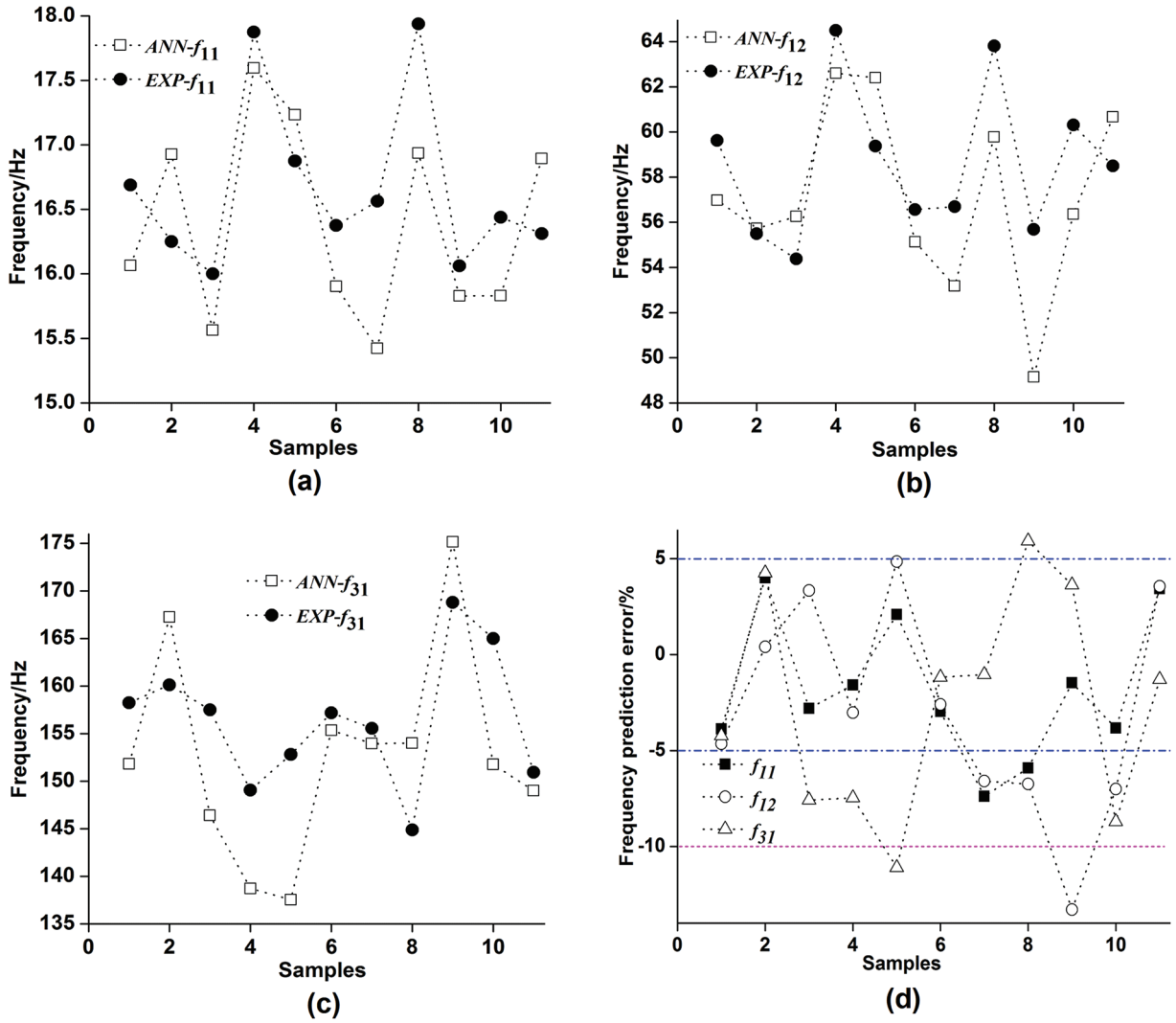

Figure 4: (a) f_{11} from ANN prediction and experiment; (b) f_{12} from ANN prediction and experiment; (c) f_{31} from ANN prediction and experiment; (d) Errors of f_{11}, f_{12} and f_{31} between ANN and experiment

predicted values of f_{11}, f_{12} and f_{13}, it is noted that there errors differ between the three natural frequencies, samples and board width. The difference between experimental and predicted frequencies is within the range of 0.23 Hz–1.14 Hz for f_{11}, and 0.23 Hz to 6.53 Hz for f_{12}, 1.6 Hz to 15.27 Hz for f_{31}. The average errors of the three frequencies are 0.58 Hz, 2.85 Hz and 7.76 Hz, respectively. The predicted f_{11} and f_{12} agree well with the predicted values. However it has been shown that f_{31} is more difficult to predict accurately.

Fig. 4d shows the three frequencies prediction percent errors. It can be seen that, for the eleven validation samples, the average deviation of the frequencies is 3.58%, 5.1% and 5.13% for f_{11}, f_{12} and f_{13}, respectively. All errors are less than 10%, excluding two error values. For f_{11}, No errors are greater than 10%, and the maximum and minimum errors are 5.91% and 1.47%; while one prediction error is larger than 10% for f_{12}, which is 13.29%. Similar to $f_{21,}$ one error is beyond 10%, which is 11.11% for f_{31}. Regarding the panels consisting of 32 mm wide laminates (Samples 1 to 5), one panel had a prediction error of 10%, which is the same as the boards with 120 mm wide laminates (Samples 9 to 11). The prediction errors for the boards made with 76 mm wide laminates (Samples 6 to 8) were all less than 10%. In comparison with the results shown in Fig. 3, the prediction errors from this improved procedure are slightly reduced. It is likely that more training samples would help improve the accuracy of the predictions. Overall from a practical perspective, the error values reported here for the measured frequencies may be considered acceptable for online testing purposes.

4 Conclusions

Based on vibration tests performed in this study on single-layer laminated wood panels, it was found that the characteristics of the vibration signals could be extracted by three-layer decomposition procedure using wavelet packet. An ANN model was developed based on training data from 44 panels, which could be employed to generate the relationship between vibration signals and the target natural frequencies of a panel. Using a verification sample of eleven panels, it was found that the average prediction error is 4.6% for 33 predicted frequencies; only two errors were above 10% (the maximum error of 13.29%). The results demonstrate that training samples are critical for the generalization of the network model. It is concluded that the proposed method to analyze vibration test data can be utilized to evaluate full-size wood-based panel products online, such as cross laminated timber. Further research will be required to refine the vibration test techniques.

Author Contributions: Conceptualization, Jianping Sun, Jan Niederwestberg and Ying Hei Chui; Data curation, Jianping Sun, Jan Niederwestberg and Fangchao Cheng; Formal analysis, Jianping Sun and Ying Hei Chui; Funding acquisition, Jianping Sun and Ying Hei Chui; Investigation, Jianping Sun, Jan Niederwestberg and Ying Hei Chui; Methodology, Jianping Sun, Jan Niederwestberg and Fangchao Cheng; Project administration, Jianping Sun and Ying Hei Chui; Resources, Jianping Sun, Jan Niederwestberg and Ying Hei Chui; Supervision, Jan Niederwestberg and Ying Hei Chui; Validation, Jan Niederwestberg and Ying Hei Chui; Writing—original draft, Jianping Sun; Writing—review & editing, Jan Niederwestberg and Ying Hei Chui.

Funding Statement: This research was supported by National Natural Science Foundation of China (Project No. 31660174), Guangxi Innovation-Driven Development Special Fund Project of China (Project No. AA17204087-16) and through funding to NSERC Strategic Network on Innovative Wood Products and Building System, by the Natural Sciences and Engineering Research Council of Canada.

Conflicts of Interest: The authors declare that they have no conflicts of interest to report regarding the present study.

References

1. United Nations Economic Commission for Europe. (2020). *Forest products annual market review 2018-2019*. *S.l.*: United Nations.
2. Gong, Y. C., Liu, F. L., Tian, Z. P., Wu, G. F., Ren, H. Q. et al. (2019). Evaluation of mechanical properties of cross-laminated timber with different lay-ups using Japanese larch. *Journal of Renewable Materials, 7(10),* 941–956. DOI 10.32604/jrm.2019.07354.
3. Li, Y., Lam, F. (2016). Reliability analysis and duration-of-load strength adjustment factor of the rolling shear strength of cross laminated timber. *Journal of Wood Science, 62(6),* 492–502. DOI 10.1007/s10086-016-1577-0.
4. Pang, S. J., Jeong, G. Y. (2019). Effects of combinations of lamina grade and thickness, and span-to-depth ratios on bending properties of cross-laminated timber (CLT) floor. *Construction and Building Materials, 222,* 142–151. DOI 10.1016/j.conbuildmat.2019.06.012.
5. American Society of Testing Materials (ASTM) International. (2015). *ASTM D198-15, Standard Test Methods of Static Tests of Lumber in Structural Sizes*.
6. ANSI. (2018). *Standard for performance-rated cross laminated timber*. *ANSI/APA PRG 320-2018*. Washington, DC: American National Standards Institute.
7. Senalik, C. A., Zhou, L., Ross, R. J. (2017). Assessment of deterioration in timbers with time and frequency domain analysis techniques. In: Wang, X., Senalik, C. A., Ross, R. J. eds. *Proceedings, 20th International Nondestructive Testing and Evaluation of Wood Symposium. Gen. Tech. Rep. FPL-GTR-249*. Madison, WI: US Department of Agriculture, Forest Service, Forest Products Laboratory: 298-310. (Vol. 249, pp. 298–306).
8. Lin, C., Cho, C., Yang, T. (2012). Investigation on the fundamental properties of cross-laminated timber (CLT) using nondestructive methods. *IUFRO Conference Division 5 Forest Products,* Estoril, Lisbon, Portugal, 8-13 July 2012.
9. Lin, C. H., Li, J. R., Yang, T. H. (2015). Evaluation on the physical and mechanical properties of Japanese cedar cross-laminated timber flooring. *Forest Products Industry, 34(1),* 1–10.
10. Ido, H., Nagao, H., Harada, M., Kato, H., Ogiso, J. et al. (2016). Effects of the width and lay-up of sugi cross-laminated timber (CLT) on its dynamic and static elastic moduli, and tensile strength. *Journal of Wood Science, 62(1),* 101–108. DOI 10.1007/s10086-015-1527-2.
11. Anthonie, K. A., Barbosa, A. R., Sinha, A. (2014). Viability of hybrid poplar in ANSI approved cross-laminated timber applications. *Journal of Materials in Civil Engineering, 26(7),* 1–5. DOI 10.1061/(ASCE)MT.1943-5533.0000778.
12. Concu, G., Fragiacomo, M., Trulli, N., Valdes, M. (2017). Nondestructive assessment of gluing in cross-laminated timber panels. *Sustainable Development and Planning IX, 226,* 559–569.
13. Gülzow, A., René Steiger, R., Gsell, D. (2010). Nondestructive evaluation of stiffness properties of cross-laminated solid wood panels. *11th World Conference on Timber Engineering WCTE,* Riva del Garda, Italy.
14. Larsson, D. (1997). Using modal analysis for estimation of anisotropic material constants. *Journal of Engineering Mechanics, 123(3),* 222–229. DOI 10.1061/(ASCE)0733-9399(1997)123:3(222).
15. Mai, K. Q., Park, A., Nguyen, K. T., Lee, K. (2018). Full-scale static and dynamic experiments of hybrid CLT–concrete composite floor. *Construction and Building Materials, 170,* 55–65. DOI 10.1016/j.conbuildmat.2018.03.042.
16. Saul, A., Maldonado, H., Chui, Y. H. (2012). Vibration properties of cross laminated timber floors. *13th World Conference on Timber Engineering,* Auckland, New Zealand.
17. Mugabo, I., Barbosa, A. R., Riggio, M., Batti, J. (2019). Ambient vibration measurement data of a four-story mass timber building. *Frontiers in Built Environment, 5(67),* 1–4. DOI 10.3389/fbuil.2019.00001.
18. Mugabo, I., Barbosa, A. R., Riggio, M. (2019). Dynamic characterization and vibration analysis of a four-story mass timber building. *Frontiers in Built Environment, 5(86),* 1–16. DOI 10.3389/fbuil.2019.00001.
19. Deobald, L. R., Gibson, R. F. (1988). Determination of elastic constants of orthotropic plates by a modal analysis/Rayleigh-Ritz technique. *Journal of Sound and Vibration, 124(2),* 269–283. DOI 10.1016/S0022-460X(88)80187-1.

20. Leissa, A. W. (1993). *Vibration of plates*. *Reprinted edition*. Acoustical Society of America. Originally issued by NASA in 1973 (published 1969). Washington DC, USA.
21. Sobue, N., Katoh, A. (1992). Simultaneous determination of orthotropic elastic constants of standard full-size plywoods by vibration method. *Mokuzai Gakkaishi, 38,* 895–902.
22. Gsell, D., Feltrin, G., Schubert, S., Steiger, R., Motavalli, M. (2007). Cross-laminated timber plates: evaluation and verification of homogenized elastic properties. *Journal of Structural Engineering, 133(1),* 132–138. DOI 10.1061/(ASCE)0733-9445(2007)133:1(132).
23. Steiger, R., Gülzow, A., Gsell, D. (2008). Non-destructive evaluation of elastic material properties of cross-laminated timber (CLT). *Conference Cost E53, 29-30 October 2008,* Delft, The Netherlands.
24. Czaderski, C., Steiger, R., Howald, M., Olia, S., Gülzow, A. et al. (2007). Versuche und Berechnungen an allseitig gelagerten 3-schichtigen Brettsperrholzplatten. *Holzforschung, 65,* 383–402.
25. Steiger, R., Gülzow, A., Czaderski, C., Howald, M. T., Niemz, P. (2012). Comparison of bending stiffness of cross-laminated solid timber derived by modal analysis of full panels and by bending tests of strip-shaped specimens. *European Journal of Wood and Wood Products, 70(1-3),* 141–153. DOI 10.1007/s00107-011-0521-7.
26. Zhou, J., Chui, Y. H., Gong, M., Hu, L. (2017). Comparative study on measurement of elastic constants of wood-based panels using modal testing: choice of boundary conditions and calculation methods. *Journal of Wood Science, 63(5),* 523–538. DOI 10.1007/s10086-017-1645-0.
27. Zhou, J., Chui, Y. H., Gong, M., Hu, L. (2017). Elastic properties of full-size mass timber panels: characterization using modal testing and comparison with model predictions. *Composites Part B: Engineering, 112,* 203–212. DOI 10.1016/j.compositesb.2016.12.027.
28. Chui, Y. H., Smith, I. (1990). Influence of rotatory inertia, shear deformation and support condition on natural frequencies of wooden beams. *Wood Science and Technology, 24(3),* 233–245. DOI 10.1007/BF01153557.
29. Chui, Y. H. (1991). Simultaneous evaluation of bending and shear moduli of wood and the influence of knots on these parameters. *Wood Science and Technology, 25(2),* 125–134. DOI 10.1007/BF00226812.
30. Niederwestberg, J., Chui, Y. H. (2012). Characterizing influence of laminate characteristics on elastic properties of single layer in cross laminated timber. *Proceedings of World Conference in Timber Engineering, Auckland*. *7,* 130–135.